arXiv:1402.0519v2 [physics.atom-ph] 11 Feb 2014

# $K$-Shell Photoionization of B-like Atomic Nitrogen Ions: Experiment and Theory

**M F Gharaibeh[1], N El Hassan[2]‡, M M Al Shorman[2], J M Bizau[2,3]†, D Cubaynes[2,3], S Guilbaud[2], I Sakho[4], C Blancard[5] and B M McLaughlin[6,7]§**

[1]Department of Physics, Jordan University of Science and Technology, Irbid 22110, Jordan
[2]Institut des Sciences Moléculaires d'Orsay (ISMO), CNRS UMR 8214, Université Paris-Sud, Bât. 350, F-91405 Orsay cedex, France
[3]Synchrotron SOLEIL - L'Orme des Merisiers, Saint-Aubin - BP 48 91192 Gif-sur-Yvette cedex, France
[4]Department of Physics, UFR of Sciences and Technologies, University Assane Seck of Ziguinchor, Ziguinchor, Senegal
[5]CEA-DAM-DIF, Bruyères-le-Châtel, F-91297 Arpajon Cedex, France
[6]Centre for Theoretical Atomic, Molecular and Optical Physics (CTAMOP), School of Mathematics and Physics, The David Bates Building, 7 College Park, Queen's University Belfast, Belfast BT7 1NN, UK
[7]Institute for Theoretical Atomic and Molecular Physics (ITAMP), Harvard Smithsonian Center for Astrophysics, MS-14, Cambridge, MA 02138, USA

**Abstract.** Measurements of absolute cross sections for the $K$-shell photoionization of B-like atomic nitrogen ions were carried out utilizing the ion-photon merged-beam technique at the SOLEIL synchrotron radiation facility in Saint-Aubin, France. High-resolution spectroscopy with $E/\Delta E \approx 13{,}500$ was the maximum resolution achieved. We have investigated two photon energy regions: 404 eV – 409 eV and 439 eV – 442 eV. Resonance peaks found in the experimental measured cross sections are compared with theoretical estimates from the multi-configuration Dirac - Fock, R-matrix and empirical methods, allowing identification of the strong 1s $\rightarrow$ 2p and the weaker 1s $\rightarrow$ 3p resonances in the observed $K$-shell spectra of this B-like nitrogen ion.

PACS numbers: 32.80.Fb, 31.15.Ar, 32.80.Hd, and 32.70.-n

Short title: $K$-shell photoionization of B-like atomic nitrogen ions

Submitted to: *J. Phys. B: At. Mol. Opt. Phys. : 12 February 2014*

‡ Present address: Laboratoire Structures, Propriétés et Modélization des Solides (SPMS) UMR CNRS 8580, Ecole Centrale Paris, 1, Grande Voie des Vignes, 92295 Châtenay-Malabry, France
† Corresponding author, E-mail: jean-marc.bizau@u-psud.fr
§ Corresponding author, E-mail:b.mclaughlin@qub.ac.uk

## 1. Introduction

X-ray spectra from *XMM-Newton* may be utilized to characterize the interstellar medium (ISM), if accurate atomic $K$-edge cross sections are available [1, 2, 3, 4, 5, 6, 7]. Single and multiply ionization stages of C, N, O, Ne and Fe have been observed in the ionized outflow in NGC 4051 measured with *XMM-Newton* [8] in the soft x-ray region and low ionized stages of C, N and O have also been used in modelling x-ray emission from OB super-giants [9]. Radiative/photo recombination of singly and doubly charged nitrogen ions also play an important role in the chemistry of the atmosphere of Titan [10]. Detailed photoionization models of the brightest knot of star formation in the blue compact dwarf galaxy Mrk 209 required abundances for ions of oxygen and nitrogen [11]. The XMM-*Newton* X-ray spectra of WR 1 is rich in nitrogen ions [12] and photoionization cross section data and abundances for carbon, nitrogen, and oxygen in their various stages of ionization are essential for photoionization models applied to the plasma modelling in a variety of planetary nebulae [13]. In the present study we focus our attention on obtaining detail spectra on the doubly ionized nitrogen ion $N^{2+}$ (N III) in the vicinity of its $K$ - edge.

Photoionization (PI) cross sections used for the modelling of astrophysical phenomena have mainly been provided by theoretical methods, due to limited experimental data being available. Major effort has gone into improving the quality of calculated data using state-of-the-art theoretical methods. Recent advances in the determination of atomic parameters for modeling $K$ lines in cosmically abundant elements have been reviewed by Quinet and co-workers [4].

Absolute experimental $K$-shell photoionization cross section results have been obtained by various groups on a variety of atoms and ions of astrophysical interest; He-like $Li^+$ [14, 15, 16], Li-like $B^{2+}$ [17], $C^{3+}$ [18], $N^{4+}$ [6], Be-like $B^+$ [19], $C^{2+}$ [20], $N^{3+}$ [6], B-like $C^+$ [21], C-like $N^+$ [5], N-like $O^+$ [22], F-like $Ne^+$ [23], neutral nitrogen [24] and oxygen [25, 26, 27, 28].

Recent studies on $K$-shell photoionization cross sections calculations for neutral nitrogen and oxygen showed excellent accord with high resolution measurements made at the Advanced Light Source (ALS) radiation facility [24, 28] as have similar cross section calculations on singly and multiply ionized stages of atomic nitrogen compared with high resolution measurements at the SOLEIL synchrotron facility [5, 6]. The majority of the high-resolution experimental data from third generation light sources have been shown to be in excellent agreement with the state-of-the-art R-matrix method [29, 30] and with other modern theoretical approaches.

The present investigation for this proto-type B-like atomic nitrogen ion gives accurate values of photoionization cross sections produced by x-rays in the vicinity of the $K$-edge, where strong n=2 inner-shell resonance states of $N^{2+}$ are observed. This work compliments our previous studies on $K$-shell photoionization of singly and multiply ionized atomic nitrogen ions [5, 6] in the vicinity of the K-edge. Previous experimental studies on B-like atomic nitrogen have been performed only in the valence shell region [31, 32]. To date no experimental studies for the $K$-edge region have been reported in the literature. For the B-like ions $N^{2+}$, $O^{3+}$ and $F^{4+}$, absolute experimental cross section measurements in the near threshold region were made by Bizau and co-workers [31, 32]. Close-coupling calculations performed by Li-Guo and Xin-Xiao [33] based on the R-matrix formalism [34] obtained excellent agreement with the experimental work of Bizau and co-workers [32]. In this near threshold region it was necessary to include both the ground state and metastable excited states in the

theoretical work in order to achieve suitable agreement with experiment.

We follow a similar approach here for the *K*-shell energy region. $N^{2+}$ ions produced in the SOLEIL synchrotron radiation experiments are not purely in their ground state. *K*-shell photoionization contributes to the ionization balance in a more complicated way than outer shell photoionization. In fact *K*-shell photoionization when followed by Auger decay couples three or more ionization stages instead of two in the usual equations of ionization equilibrium [35].

The 1s → 2p photo-excitation process on the $1s^2 2s^2 2p\ ^2P^o$ ground-state of B-like nitrogen ion is,

$$h\nu + N^{2+}(1s^2 2s^2 2p\ ^2P^o) \rightarrow N^{2+}\ (1s2s^2\ 2p^2[^3P,^1D,^1S]\ ^2S,^2P,^2D)$$

which can decay to

$$\swarrow \quad \searrow$$

$$N^{3+}\ (1s^2 2s^2\ ^1S) + e^-(k_\ell^2),\ \text{ or }\ N^{3+}\ (1s^2 2s\ np\ ^1P^\circ) + e^-(k_\ell^2),$$

where $k_\ell^2$ is the outgoing energy of the continuum electron with angular momentum $\ell$. Experimental studies on this doubly ionized atomic nitrogen ion, in its ground state $1s^2 2s^2 2p\ ^2P^o$, are also hampered by metastable states present in the parent ion beam. In the present experimental studies performed at the SOLEIL radiation facility, $N^{2+}$ ions are produced in the gas-phase using an Electron-Cyclotron-Resonance-Ion-Source (ECRIS) so the metastable state $1s^2 2s2p^2\ ^4P$ can be present in the parent ion beam.

For the $1s^2 2s2p^2\ ^4P$ metastable state, auto-ionization processes occurring by the 1s → 2p photo-excitation process are mainly;

$$h\nu + N^{2+}(1s^2 2s2p^2\ ^4P)$$

$$\downarrow$$

$$N^{2+}[1s2s[^{1,3}S]\,2p^3(^4S^o,^2D^o,^2P^o)]^4S^o,^4P^o,^4D^o$$

$$\downarrow$$

$$N^{3+}(1s^2 2s\ np\ ^3P^o) + e^-(k_\ell^2).$$

In the vicinity of the *K*-edge our current investigations appear to be the first time this B-like system has been studied experimentally for such an energy region.

State-of-the-art *ab initio* calculations for Auger inner-shell processes were first carried out on this B-like system by Petrini and de Araújo [35] using the R-matrix method [29] and followed a similar procedure to the work on *K*-shell studies for the Be-like $B^+$ ion [36]. Stoica and co-workers [37] noted that once the 1s-hole was created in the ions, by single photoionization, with simultaneous shake-up and shake-off processes, Auger decay populates directly excited states of the residual ions, which then produces UV lines. This work was further extended by Garcia and co-workers [38], using the optical potential method within the Breit-Pauli R-matrix formalism [29, 30, 39, 34], for photoionization of the ground state only, along the nitrogen iso-nuclear sequence. Garcia and co-workers [38] pointed out that the earlier central field calculations [40, 41, 42] did not account for the strong autoionizing resonance features that dominate the cross sections near the *K*-edge.

In the present study we compare our theoretical cross section results from the multi-configuration Dirac Fock (MCDF) and R-matrix methods with previous theoretical results [43, 44, 38] and with the current experimental measurements made

at the SOLEIL synchrotron radiation facility. Detailed measurements of the *K*-shell single photon ionization cross sections for B-like nitrogen ions, were made in the 404 eV – 409 eV region (where strong peaks were observed) and in the photon energy range 439 eV – 442 eV. The results for resonance energies and Auger widths are compared with detailed theoretical predictions made using the MCDF [45], R-matrix [34] and the SCUNC empirical methods [46, 47]. The theoretical predictions assist in the identification and characterization of the strong 1s $\rightarrow$ 2p and the weaker 1s $\rightarrow$ 3p resonances observed in the B-like nitrogen spectra. The current study gives absolute values (experimental and theoretical) for PI cross sections along with n=2 and n=3 inner-shell resonance energies, natural line widths and resonance strengths, for the situation of a photon interacting with the ground $1s^2 2s^2 2p\ ^2P^o$, and metastable $1s^2 2s 2p^2\ ^4P$ states of the $N^{2+}$ ion.

In section 2 we briefly outline the experimental procedure used and section 3 presents the theoretical procedures used. Section 4 gives a discussion of our experimental and theoretical results. Finally in section 5 conclusions are drawn from the present study.

## 2. Experiment

Cross sections for photoionization of B-like atomic nitrogen ions were measured in the range where *K*-shell photoionization occurs. The experiment was performed at the MAIA (Multi-Analysis Ion Apparatus) set-up, permanently installed on branch A of the PLEIADES beam line [48, 49] at SOLEIL, the French National Synchrotron Radiation Facility, located in Saint–Aubin, France. Further details of the experimental setup were outlined in our previous publications on $N^+$ [5], $N^{3+}$ and $N^{4+}$ [6] therefore only a brief summary will be given here. The $N^{2+}$ ions are produced in a permanent magnet electron cyclotron resonance ion source (ECRIS). Collimated $N^{2+}$ ion-beam currents up to 160 nA were extracted from the ion source after biasing the ion source by +2 kV and then selected by mass per charge ratio using a dipole magnet selector. The ion beam was placed on the same axis as the photon beam by using electrostatic deflectors and einzel lenses to focus the beam. After the interaction region between the photon and the ion beams, another dipole magnet separates the primary beam and the beam of ions which have gained one (or several) charge(s) in the interaction, the so-called photo-ions. The primary ions are collected in a Faraday cup and the photon-ions are detected by multi-channel plates detector. The photon current is measured by a calibrated photodiode. Ions with the same charge as the photo-ions can also be produced by collisions between the primary ions and the residual gas or stripping on the walls in the interaction region. This background signal is subtracted by chopping the photon beam, collecting the data with and without photons for 20 seconds accumulation time.

For the absolute measurements of the PI cross sections, a -1000 V bias is applied on the 50 cm long interaction-region and the data are collected with 30 meV photon energy steps. The overlap of the two beams and the density distributions of the interacted particles is determined in three dimensions by using three sets of scanning slits. The cross sections obtained have an estimated systematic uncertainty of 15%. In another spectroscopy mode, no bias is applied to the interaction region allowing the photon and ion beams to interact over about 1 m and to scan the photon energy with a finer step. In this mode, only relative cross sections can be measured. They are later normalized on the cross sections determined in the absolute mode assuming the area

under the resonances to be the same. The energy and band width of the photon beam are calibrated separately using a gas cell and $N_2$ ($1s \rightarrow \pi^*_g$ v=0) photoionization lines, located at 400.87 eV [50] and Ar $2p_{3/2}{}^{-1}4s$ at 244.39 eV [51]. The photon energy, once corrected for Doppler shift, has an uncertainty of approximately 30 meV. The relative uncertainty on the band passes is of the order of 10 %. Outstanding possibilities in terms of spectral resolution and flux at the $N_2$ ($1s^{-1}$) $K$-edge have been discussed recently by Miron and co-workers [52, 53].

## 3. Theory

### *3.1. SCUNC: B-like nitrogen*

In the framework of the Screening Constant by Unit Nuclear Charge (SCUNC) formalism [46, 47], the total energy of the core-excited states is expressed in the form given by,

$$E\left(N\ell n\ell';^{2S+1}L^{\pi}\right) = -Z^2\left[\frac{1}{N^2}+\frac{1}{n^2}\left[1-\beta\left(N\ell n\ell';^{2S+1}L^{\pi};Z\right)\right]^2\right] \quad (1)$$

where $E\left(N\ell n\ell';^{2S+1}L^{\pi}\right)$ is in Rydberg units. In this equation, the principal quantum numbers $N$ and $n$ are respectively for the inner and the outer electron of the He-like iso-electronic series. The $\beta$-parameters are screening constants by unit nuclear charge expanded in inverse powers of $Z$ and are given by the expression,

$$\beta\left(N\ell n\ell';^{2S+1}L^{\pi}\right) = \sum_{k=1} f_k\left(\frac{1}{Z}\right)^k \quad (2)$$

where $f_k\left(N\ell n\ell';^{2S+1}L^{\pi}\right)$ are parameters that are evaluated empirically from existing experimental measurements on resonance energies. Similarly one may get the Auger widths $\Gamma$ in Rydbergs (1 Rydberg = 13.605698 eV) from the formula

$$\Gamma(\mathrm{Ry}) = Z^2\left[1-\sum_q f_q\ \left(\frac{1}{Z}\right)^q\right]^2. \quad (3)$$

The Advanced Light Source experimental measurements of Schlachter and co-workers on K-shell photoionization of B-like carbon ions [21] were used to determine the appropriate empirical parameters $f_q$ for the Auger widths.

### *3.2. MCDF: B-like Nitrogen*

Multi-configuration Dirac-Fock (MCDF) calculations were performed based on a full intermediate coupling regime in a $jj$-basis using the code developed by Bruneau [45]. Photoexcitation cross sections have been carried out for B-like atomic nitrogen ions in the region of the K-edge. Only electric dipole transitions have been computed using the length form. For this B-like atomic nitrogen ion the following initial configurations were considered: $\overline{1s}^2\overline{2s}^2\overline{2p}$ and $\overline{1s}^2\overline{2s}\ \overline{2p}^2$. In order to take account of correlation and relaxation effects, multiple orbital with the same quantum number were used. The bar over the orbital indicates that they are different for the initial and final states. In order to describe the correlation and relaxation effects, multiple orbitals with the same quantum number and the following final configurations were considered: $1s2s^22p^2$, $1s2s2p^2np$, $1s2s2p^3$, $1s2s^22pnp$. Such notation means that radial functions with principal quantum number n =1 or 2 are not the same for initial and final

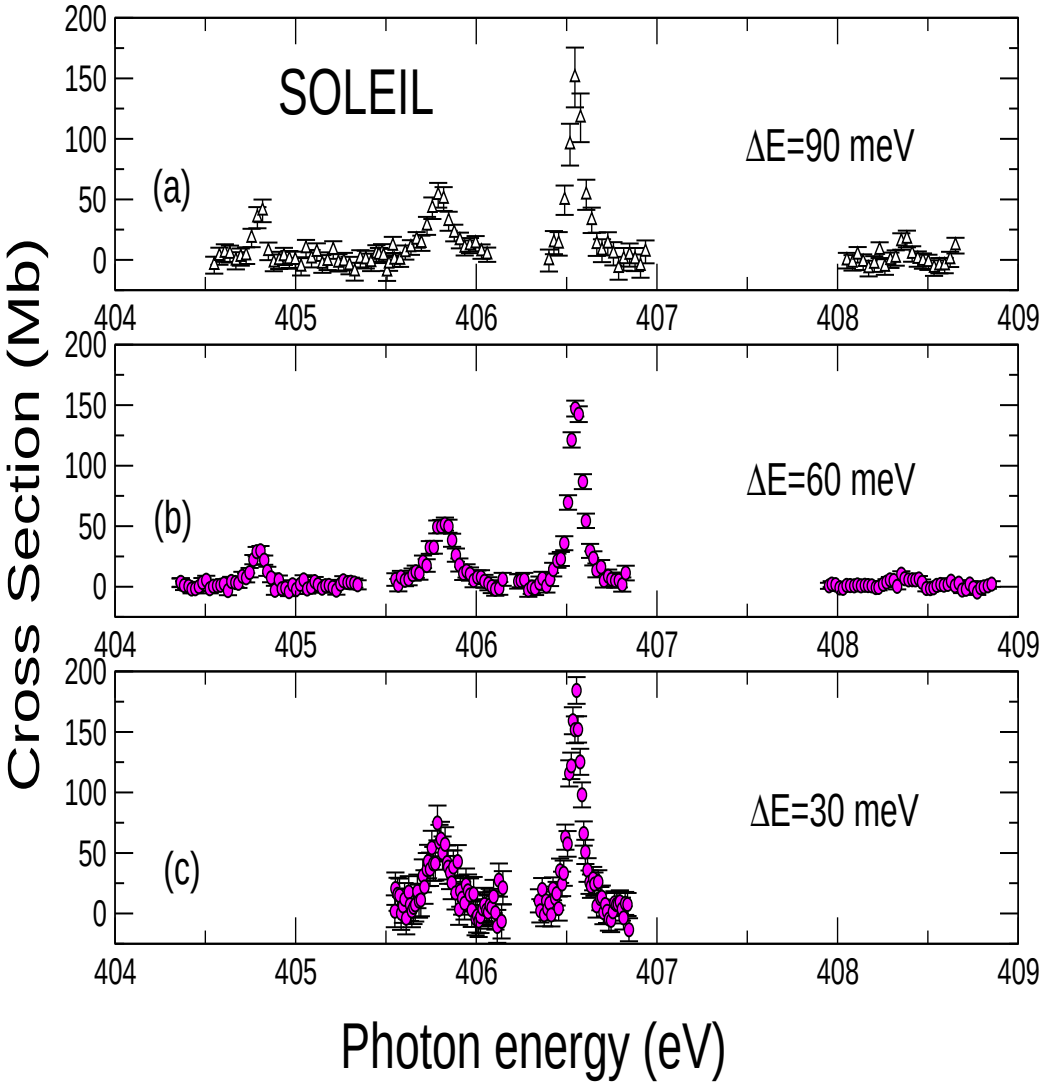


**Figure 1.** (Colour online) Experimental K-shell photoionization cross sections for $N^{2+}$ ions measured with various band passes at the SOLEIL synchrotron radiation facility over the photon energy region 404 eV - 409 eV. (a) absolute results taken with a band pass of 90 meV FWHM, obtained in the relative mode then normalized to the scan (a). For scan (a), the error bars give the total uncertainty, and the statistical uncertainty for scans (b) and (c).

configurations. Radial functions with principal quantum number up to n=6 were included in our calculations. Photoexcitation cross sections from the $1s^2 2s^2 2p$ and $1s^2 2s 2p^2$ configurations were calculated separately. The wavefunctions were calculated minimizing the following energy functional:

$$E = \frac{\sum_\alpha (2J_\alpha + 1) E_\alpha}{2\sum_\alpha (2J_\alpha + 1)} + \frac{\sum_\beta (2J_\beta + 1) E_\beta}{2\sum_\beta (2J_\beta + 1)} \tag{4}$$

where $\alpha$ and $\beta$ run over all the initial and final states, respectively.

Synthetic spectra were constructed as a weighted sum of the photoexcitation cross sections from the ground state levels $1s^2 2s^2 2p(^2P_{1/2,3/2})$ and the metastable state levels $1s^2 2s 2p^2(^4P^\circ_{1/2,3/2,5/2})$. In order to compare with the SOLEIL experiments the weights used were 80 % of the $^2P^\circ$ levels, and 20 % for the $^4P$. Each electric dipole transition has been dressed by a Lorenztian profile with a full width half maximum (FWHM) given by the autoionization width of the upper level. The autoionization widths were evaluated from our MCDF calculations and for the photo-excited configurations $1s2s^2 2p^2$ and $1s2s2p^3$. The average Auger widths were found respectively to be 64 meV and 105 meV.

### *3.3. R-matrix: B-like Nitrogen*

The *R*-matrix method [34], implemented in a parallel version of the codes [54, 55, 56] was used to determine all the cross sections. The PI cross sections were carried out for the initial $^2P^o$ ground state and the $^4P$ metastable states. All the PI cross section calculations were performed in *LS*-coupling with 390-levels of the residual ion retained in the close-coupling expansion. The 1s, 2s and 2p tabulated orbitals from the work of Clementi and Roetti [57] were used together with n=3 physical and n=4 pseudo-orbitals of the $N^{3+}$ residual ion. The n=4 pseudo-orbitals were energy optimized on the appropriate $1s^{-1}$ hole-shell states [58], employing the atomic structure code CIV3 [59]. These n=4 so called pseudo-orbitals are incorporated into the scattering basis set to try and accommodate for core relaxation and electron correlation effects in the multi-reference-configuration interaction wavefunctions used to describe the atomic ion states. All the $N^{3+}$ residual ion states were then represented by using multi-reference-configuration-interaction (MRCI) wave functions. The non-relativistic *R*-matrix approach was used to calculate the energies of the $N^{2+}$ bound states and the subsequent PI cross sections.

The R-matrix with pseudo-states method (RMPS) was used to determine all the cross sections (in *LS* - coupling) with 390 levels of the $N^{3+}$ residual ion included in the close-coupling calculations. Since metastable states are present in the parent ion beam, theoretical PI cross-section calculations are required for both the $1s^2 2s^2 2p\ ^2P^o$ ground state and the $1s^2 2s 2p^2\ ^4P$ metastable states of the $N^{2+}$ ion for a proper comparison with experiment.

The scattering wavefunctions were generated by allowing two-electron promotions out of selected base configurations of $N^{2+}$. Scattering calculations were performed with twenty continuum functions and a boundary radius of 9.4 Bohr radii. For the $^2P^o$ ground state and the $^4P$ metastable states the electron-ion collision problem was solved with a fine energy mesh of $2\times10^{-7}$ Rydbergs ($\approx 2.72\ \mu$eV) to delineate all the resonance features in the PI cross sections. Radiation and Auger damping were also included in the cross section calculations.

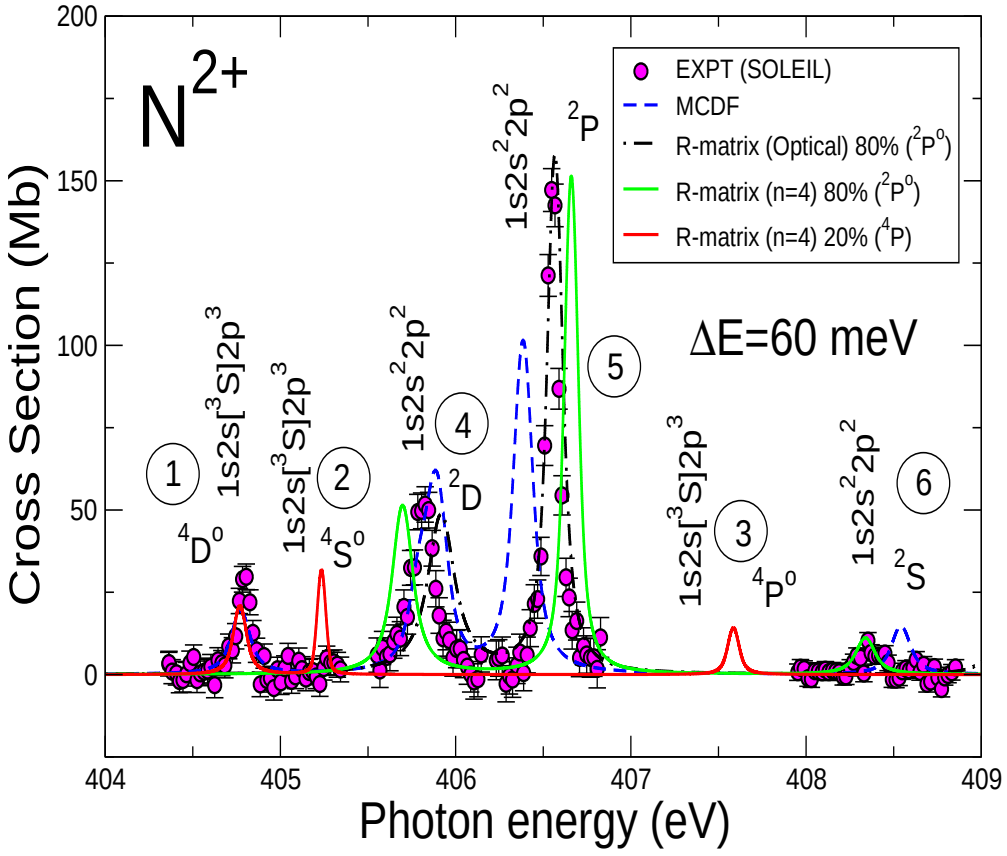


**Figure 2.** (Colour online) Photoionization cross sections for $N^{2+}$ ions measured with a 60 meV band pass at SOLEIL. Solid circles : total photoionization. The error bars give the statistical uncertainty of the experimental data. The MCDF (dashed line), R-matrix RMPS (solid line, red, $^4$P, green, $^2$P$^o$), and the Optical potential (dash-dot line, $^2$P$^o$ only) [38] calculations shown were obtained by convolution with a Gaussian distribution having a profile width at FWHM of 60 meV and a weighting of the ground and metastable states (see text for details) to simulate the measurements. Tables 1 and 2 gives the designation and the parameters of the resonances ① - ⑥ in this photon energy region.

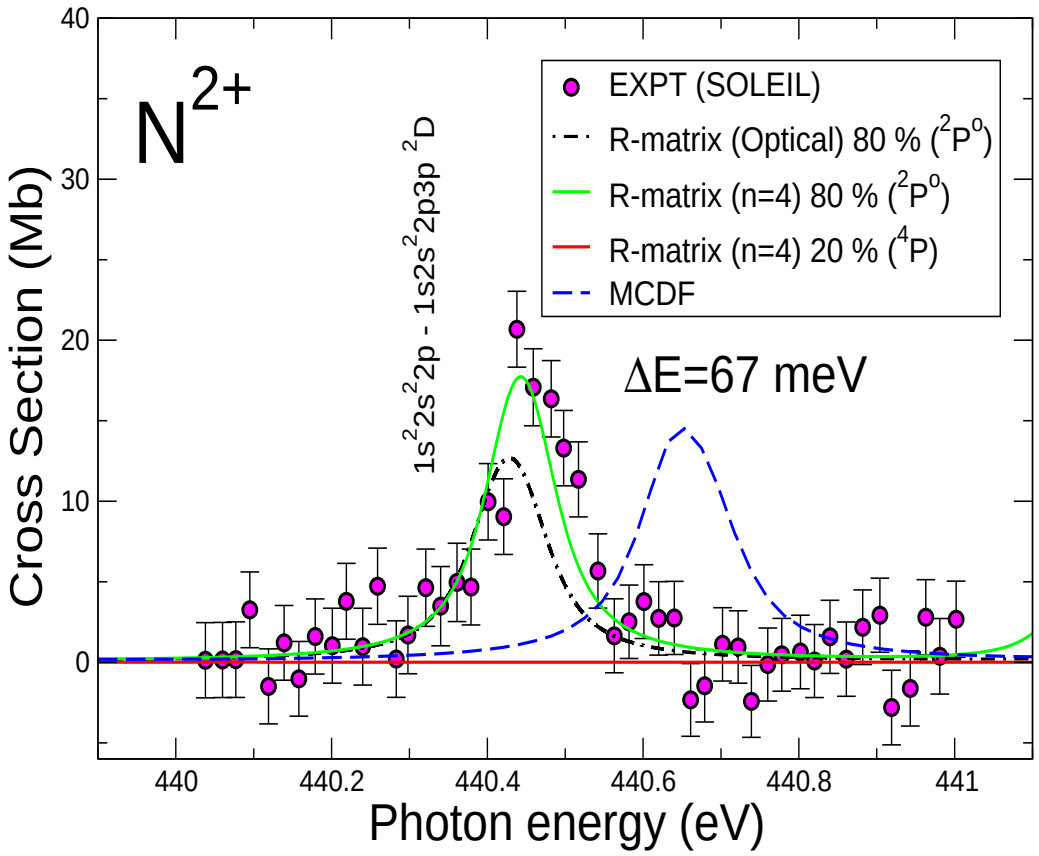


**Figure 3.** (Colour online) Photoionization cross sections for $N^{2+}$ ions measured with a 67 meV FWHM band pass at the SOLEIL radiation facility. Solid circles : total cross sections. The error bars give the statistical uncertainty of the experimental data. The MCDF (dashed line, blue), R-matrix RMPS (solid line, red $^4$P, green $^2$P$^o$) and the Optical potential (dash-dot line, $^2$P$^o$ only) [38] calculations shown were obtained by convolution with a Gaussian distribution having a profile width at FWHM of 67 meV and a weighting of the ground and metastable states (see text for details) to simulate the measurements.

For a direct comparison with the SOLEIL results, the R-matrix cross section calculations were convoluted with a Gaussian function of appropriate width and an admixture of 80% ground and 20 % metastable states used to best simulate experiment.

The peaks found in the theoretical photoionization cross section spectrum were fitted to Fano profiles for overlapping resonances [60, 61, 62] as opposed to the energy derivative of the eigenphase sum method [63, 64, 65]. The theoretical values for the natural linewidths $\Gamma$ determined from this procedure are presented in Tables 1 and 2 and compared with results obtained from the high-resolution SOLEIL synchrotron measurements and with other theoretical methods.

R-matrix calculations were also performed using an n=2 basis (1s, 2s and 2p) comparable to the work of Garcia and co-workers [38] for the $^4$P metastable. The appropriate resonance parameters (for the $^4$P metastable and the $^2$P$^o$ ground state similar to the work of Garcia and co-workers [38]) are included in Tables 1 and 2 from these calculations for completeness.

## 4. Results and Discussion

Over the two photon energy ranges investigated we found in the cross sections that the most intense resonance peaks were located in the photon energy region, 404 eV – 409 eV. All the experimental measurements are shown in figure 1, taken at the various spectral photon energy resolutions, ranging from 30 meV to 90 meV at FWHM. We note that since the $^4$P metastable state of the $N^{2+}$ ion is present in the parent experimental beam, theory may be used to estimate its content. Figure 2 shows our experimental and theoretical (MCDF and R-matrix) results for the restrictive photon energy range of 404 eV – 409 eV. From our theoretical R-matrix studies on this system we find that an admixture of 80% ground state and 20 % metastable state in the parent ion beam indicates satisfactory agreement between theory and experiment. This admixture was determined by comparing the area under the strong peaks between experiment and theory.

For a direct comparison with the experimental work both the MCDF and R-matrix theoretical cross sections were convoluted with a Gaussian distribution function having a profile width at FWHM of 60 meV and the above admixture used to simulate the SOLEIL measurements and the results presented in figure 2. Figure 2 illustrates the experimental and theoretical (MCDF and R-matrix) single photonionization cross sections results over the photon energy range from 404 eV – 409 eV at the energy resolution of 60 meV. Tables 1 and 2 gives the experimental and theoretical estimates for all of the resonance parameters of the peaks located in the photon energy range 404 eV - 409 eV. From Table 2, one sees that the MCDF predictions for the $^2$S resonance energy is at 410.1 eV, outside of the energy range investigated. The peaks found in the photoionization cross section spectra measured at SOLEIL for this B-like atomic nitrogen were fitted to Voigt functions. Voigt profiles were used to fit the peaks in the experimental data, in order to extract the line widths, with a Gaussian instrumental profile of 60 meV assumed for each peak. For the determination of the experimental widths, each individual sweep has been fitted separately by Voigt profiles to avoid any possible shift in the energy delivered by the monochromator. Then the final width of the Lorentzian component was obtained from the weighted mean of the individual Lorentzian width determined from each fit. For the $N^{2+}$ ion, splitting of the $J$ components of the initial state [66] was also taken into account, assuming a statistical distribution of the levels. The experimental uncertainties in the tables are

**Table 1.** B-like atomic nitrogen ions, quartet core-excited states. Comparison of the present experimental and theoretical results for the resonance energies $E_{\rm ph}^{\rm (res)}$ (eV), natural linewidths $\Gamma$ (meV) and resonance strengths $\overline{\sigma}^{\rm PI}$ (in Mb eV), for the dominant core photoexcited n=2 states of the $N^{2+}$ ion, in the photon energy region 404 eV to 409 eV with previous investigations.

| Resonance (Label) | | SOLEIL (Experiment†) | R-matrix (Theory) | MCDF/Others (Theory) |
|---|---|---|---|---|
| $1s2s[^3S]2p^3\ ^4D^\circ$ ① | $E_{\rm ph}^{\rm (res)}$ | 404.794 ± 0.03† | 404.776[a] | 404.784[b] |
| | | | 404.623[e] | 405.630[c] |
| | | | | 404.930[d] |
| | $\Gamma$ | 56 ± 19 | 62[a] | |
| | | | 68[e] | 31[c] |
| | | | | 56[d] |
| | $\overline{\sigma}^{\rm PI}$ | 3.21 ± 0.74 | 2.53[a] | – |
| $1s2s[^3S]2p^3\ ^4S^\circ$ ② | $E_{\rm ph}^{\rm (res)}$ | – | 405.234[a] | 405.780[b] |
| | | | 405.553[e] | 404.354[c] |
| | | | | 405.510[d] |
| | $\Gamma$ | – | 15[a] | – |
| | | | 16[e] | 12[c] |
| | | | | 11[d] |
| | $\overline{\sigma}^{\rm PI}$ | – | 2.19[a] | – |
| $1s2s[^3S]2p^3\ ^4P^o$ ③ | $E_{\rm ph}^{\rm (res)}$ | - | 407.584[a] | 408.543[b] |
| | | | 408.273[e] | 408.411[c] |
| | | | | 407.580[d] |
| | $\Gamma$ | – | 48[a] | – |
| | | | 51[e] | 24[c] |
| | | | | 15[d] |
| | $\overline{\sigma}^{\rm PI}$ | – | 1.35[a] | – |

†SOLEIL, experimental work.
[a]R-matrix, n=4 basis, *LS*-coupling, present work.
[b]MCDF, present work
[c]MCDF, Chen and co-workers. [43, 44]
[d]Screening Constant by Unit Nuclear Charge (SCUNC) approximation, present work.
[e]R-matrix, n=2 basis, intermediate coupling, level averaged.

**Table 2.** B-like atomic nitrogen ions, doublet core-excited states. Comparison of the present experimental and theoretical results for the resonance energies $E_{\rm ph}^{\rm (res)}$ (eV), natural linewidths $\Gamma$ (meV) and resonance strengths $\overline{\sigma}^{\rm PI}$ (in Mb eV), for the dominant core photoexcited n=2 states of the $N^{2+}$ ion, in the photon energy region 404 eV to 409 eV with previous investigations.

| Resonance (Label) | | SOLEIL (Experiment†) | R-matrix (Theory) | MCDF/Others (Theory) |
|---|---|---|---|---|
| $1s2s^22p^2\ ^2D$ ④ | $E_{\rm ph}^{\rm (res)}$ | 405.814 ± 0.03† | 405.703[a] | 405.890[b] |
| | | | 405.965[e] | 406.128[c] |
| | | | – | 405.980[d] |
| | | | – | |
| | $\Gamma$ | 122 ± 19 | 122[a] | 55[c] |
| | | | 109[e] | 123[d] |
| | $\overline{\sigma}^{\rm PI}$ | 10.1 ± 1.9 | 10.44[a] | – |
| $1s2s^22p^2\ ^2P$ ⑤ | $E_{\rm ph}^{\rm (res)}$ | 406.547 ± 0.03† | 406.656[a] | 406.380[b] |
| | | | 406.387[e] | 406.404[c] |
| | | | | 406.561[d] |
| | $\Gamma$ | 58 ± 7 | 62[a] | |
| | | | 43[e] | 25[c] |
| | | | | 66[d] |
| | $\overline{\sigma}^{\rm PI}$ | 16.80 ± 2.7 | 19.32[a] | – |
| $1s2s^22p^2\ ^2S$ ⑥ | $E_{\rm ph}^{\rm (res)}$ | 408.376 ± 0.03† | 408.344[a] | 410.085[b] |
| | | | 408.297[e] | 408.087[c] |
| | | | | 408.414[d] |
| | | | | – |
| | $\Gamma$ | 120 ± 60 | 106[a] | 25[c] |
| | | | 94[e] | 132[d] |
| | $\overline{\sigma}^{\rm PI}$ | 1.18 ± 0.47 | 1.87[a] | – |

†SOLEIL, experimental work.
[a]R-matrix, n=4 basis, *LS*-coupling, present work.
[b]MCDF, present work
[c]MCDF, Chen and co-workers. [43, 44]
[d]Screening Constant by Unit Nuclear Charge (SCUNC) approximation, present work.
[e]R-matrix, n=2 basis, intermediate coupling, level averaged.

the total uncertainties.

The MCDF and R-matrix cross sections results indicate suitable agreement with experiment from matching the calculated and experimental ionization thresholds. Estimates for the resonance parameters, for the $N^{2+}$ doublet and quartet states, made using the screening constant by unit nuclear charge (SCUNC) empirical fitting approach [46, 47] can be seen to be in satisfactory agreement with the more sophisticated MCDF and R-matrix theoretical methods and experiment (c.f. Tables 1 and 2).

For the peaks found in the cross sections in the photon energy range 404 eV - 409 eV, the resonance energies and linewidths (c.f. Tables 1 and 2) all indicate suitable agreement between theory and the available experimental measurements. The n=2 intermediate doublet $1s2s^22p^2\ ^2S$, $^2P$, $^2D$ resonance states have a strong presence in the resulting photoionization spectra in the photon energy range 404 eV – 409 eV. The quartet $1s2s[^3S]2p^3\ ^4S^o$, $^4P^o$, $^4D^o$ resonances have a weaker presence in the cross sections over this same photon energy range as illustrated in figure 2. The $^4S^\circ$ peak is predicted theoretically (c.f. Table 1) but could be obscured by the $^4D^o$ resonance in the experimental spectra. The two resonances are close in experimental energies and may not be individually resolved (with the present resolution), or the $^4S^\circ$ resonance could be much weaker than predicted. Tentatively there appears some experimental indication of this weak peak around about 405.2 eV but higher statistics than that used in the present experiment would be required to resolve this feature. Similarly, missing from the present experimental measurements is the $^4P^\circ$ peak (c.f. Table 1), which is observed weakly, in analogous ALS experiments on B-like carbon ($C^+$) by Schlachter and co-workers [21]. For the $N^{2+}$ ion our theoretical predictions indicate that the $1s^22s2p^2\ ^4P \rightarrow 1s2s[^3S]2p^3(^2P)\ ^4P^o$ resonance energy is located at an energy of about 407.6 eV which is outside of the energy region scanned in the present experimental measurements.

For B-like nitrogen, from tables 1 and 2, we note that peak ① ($1s2s[^3S]2p^3\ ^4D^o$) and ⑤ ($1s2s^22p^2\ ^2P$) have comparable Auger widths of about 60 meV. Peaks ④ ($1s2s^22p^2\ ^2D$) and ⑥ ($1s2s^22p^2\ ^2S$) also have similar widths but are about a factor of two larger being around 120 meV. On physical grounds we attribute this difference due to different branching ratio's and decay mechanism's to the ground and excited states of the residual $N^{3+}$ ion. An analogy may be drawn with the decay mechanism's in higher charged B-like ions, from the recent saddle-point calculations of Sun and co-workers [67] where similar trends were found.

Due to dipole selection and Hund rules, angular momentum coupling consideration give two possible $^4S^o$ states from the $1s2s[^{1,3}S]2p^3(^4S^o)$ states as opposed to a single one from the $1s2s[^3S]2p^3(^2D^o)\ ^4D^o$ state. Highly correlated R-matrix [68] and saddle-point [69] calculations on B-like carbon confirm the earlier findings on the ordering of the quartet states by Schlachter and co-workers [21]. For the present B-like system our RMPS calculations give a similar ordering of the quartet states presented in Table 1 as in $C^+$ [21, 68, 69]. Figure 2, ilustrates all of the $N^{2+}$ doublet states predicted by theory, which are observed in this spectral range. Theoretical predictions from the MCDF and R-matrix methods show suitable agreement with experiment, apart from the location of the $^2S$ resonance in the MCDF case. For the doublet states, the R-matrix results indicate better agreement with experiment (for cross sections and resonance parameters c.f. Table 2) than other theoretical methods.

Figure 3 shows the photon energy range in the vicinity of the $1s^22s^22p\ ^2P^o \rightarrow 1s2s^22p[^3P]3p\ ^2D$ transition which occurs from the ground state of the $N^{2+}$ ion. The

SOLEIL measurements in this energy region were taken with a spectral resolution of 67 meV. To compare directly with experiment the MCDF and R-matrix calculations were convoluted with a Gaussian distribution function having a profile width at FWHM of 67 meV and weighted 80% for the ground-state and 20 % for the metastable. From figure 3 it is seen that the resonance line intensities, from the present RMPS, R-matrix calculations compare more favourably with the SOLEIL measurements. The experimental energy of this resonance was found at 440.46 ± 0.04 eV with an Auger width of 90 ± 47 meV and a strength of 3.05 ± 0.83 Mb eV. For this same resonance, R-matrix predictions give an energy of 440.441 eV, a width of 90 meV and a strength of 2.79 Mb eV. MCDF predictions give an energy of 440.652 eV with a strength of 2.91 Mb eV, while SCUNC estimates give values of 440.580 eV and 73 meV respectively for the energy and the width. It is seen that the present theoretical estimates for this resonance (position and width) are in harmony with the experimental findings. On physical grounds we note that the R-matrix with pseudo-states (RMPS) approach provide additional electron-correlation which greatly improves the residual ion target structure, the ionization potential of the system, resonance energy positions and Auger widths found in the photoionization cross-sections compared to other approaches as can be seen from the results presented in Tables 1 and 2.

We note that XMM-*Newton* X-ray spectral observations of WR 1 stars indicate the NIV ($N^{3+}$) K-edge absorption edge feature is at about 460 eV (26.954 Å) [12]. For the K-edge a value of 459 eV (27.011 Å) was quoted by Daltabuit and Cox [70], obtained from the screening constant method of Slater [71, 72], which tends to overestimate the threshold as indicated by Bethe and Salpeter [73]. We point out that similar wavelength $\lambda$ differences ($\Delta\lambda \sim 0.06$ Å ) occur between K-edge experiment, observation and theoretical estimates for atomic oxygen and its ions [28, 74]. Modern methods such as the saddle-point with complex rotation [75] give a value of 457.445 eV (27.1036 Å), relative to the NIII ($N^{2+}$) ground state for this $1s2s^22p\ ^3P^o$ hole state of NIV ($N^{3+}$) in close agreement with our R-matrix estimate of 457.441 eV (27.1038 Å). Similarly for the NIV ($N^{3+}$) $1s2s^22p\ ^1P^o$ hole state, an estimate of 461.416 eV (27.870 Å) from the saddle point method [76], is in close agreement with our R-matrix values of, 461.359 eV (26.874 Å, n=3 basis), 461.422 eV (26.868 Å, n=4 basis), and 461.317 eV (26.876 Å, n=2 basis), from the earlier work of Garcia and co-workers [38].

## 5. Conclusions

*K*-shell photoionization of B-like nitrogen ions, $N^{2+}$, has been investigated using state-of-the-art experimental and theoretical methods. High-resolution spectroscopy was able to be achieved with $E/\Delta E$ = 13,500 at the SOLEIL synchrotron radiation facility, in Saint-Aubin, France, covering the photon energy ranges; 404 eV – 409 eV and 439 eV – 442 eV. Several strong peaks are found in the cross sections in the energy regions, 404 eV - 409 eV and 439 eV – 442 eV which are identified as the 1s → 2p and 1s → 3p transitions in the $N^{2+}$ *K*-shell spectrum and assigned spectroscopically with their resonance parameters tabulated in Tables 1 and 2. For the observed peaks, suitable agreement is found between the present theoretical and experimental results both on the photon-energy scale and on the absolute cross-section scale for this prototype B-like system. The strength of the present study is the high resolution of the spectra along with theoretical predictions made using state-of-the-art MCDF, R-matrix with pseudo-states and empirical methods. The present results have been compared with high resolution experimental measurements made at the

SOLEIL synchrotron radiation facility and with other theoretical methods so would be suitable to be incorporated into astrophysical modelling codes like CLOUDY [77, 78], XSTAR [79] and AtomDB [80] used to numerically simulate the thermal and ionization structure of ionized astrophysical nebulae.

## Acknowledgments

The experimental measurements were performed on the PLEIADES beamline [48, 49], at the SOLEIL Synchrotron radiation facility in Saint-Aubin, France. The authors would like to thank the SOLEIL staff and, in particular those of the PLEIADES beam line for their helpful assistance, C Miron, Xiao-Jing Liu, E Roberts and C Nicolas. B M McLaughlin acknowledges support from the US National Science Foundation through a grant to ITAMP at the Harvard-Smithsonian Center for Astrophysics, the RTRA network *Triangle de le Physique* and a visiting research fellowship from Queen's University Belfast. I Sakho acknowledges the hospitality of the Université Paris-Sud and support from the University Assane Seck of Ziguinchor during a recent visit. We thank Dr John C Raymond and Dr Randall K Smith at the Harvard-Smithsonian Center for Astrophysics for discussions on the astrophysical applications and Dr Javier Garcia for numerical values of the cross sections [38]. The computational work was carried out at the National Energy Research Scientific Computing Center in Oakland, CA, USA, the Kraken XT5 facility at the National Institute for Computational Science (NICS) in Knoxville, TN, USA and at the High Performance Computing Center Stuttgart (HLRS) of the University of Stuttgart, Stuttgart, Germany. We thank Stefan Andersson from Cray Research for his advice and assistance with the implementation and optimization of the parallel R-matrix codes on the Cray-XE6 at HLRS. The Kraken XT5 facility is a resource of the Extreme Science and Engineering Discovery Environment (XSEDE), which is supported by National Science Foundation grant number OCI-1053575.

## References

[1] McLaughlin B M 2001 *Spectroscopic Challenges of Photoionized Plasma* (*ASP Conf. Series* vol **247**) ed Ferland, G and Savin D W (San Francisco, CA: Astronomical Society of the Pacific) p 87
[2] Foster A, Smith R, Brickhouse N, Kallman T, Witthoeft M 2010 *Space Sci. Rev.* **157** 135
[3] Kallman T R 2010 *Space Sci. Rev.* **157** 177
[4] Quinet P, Palmeri P, Mendoza C, Bautista M, Garcia J, Witthoeft M, Kallman T R 2011 *J Elect. Spec. and Relat. Phenom.* **184** 170
[5] Gharaibeh M F, Bizau J M, Cubaynes D, Guilbaud S, Hassan N El, Shorman M M Al, Miron C, Nicolas C, Robert E, Blancard C and McLaughlin B M 2011 *J. Phys. B: At. Mol. Opt. Phys.* **44** 175208
[6] Shorman M M Al, Gharaibeh M F, Bizau J M, Cubaynes D, Guilbaud S, Hassan N El, Miron C, Nicolas C, Robert E, Sakho I, Blancard C and McLaughlin B M 2013 *J. Phys. B: At. Mol. Opt. Phys.* **46** 195701
[7] McLaughlin B M and Ballance C P 2013 Photoionization, Fluorescence and Inner-shell Processes *McGraw-Hill Yearbook of Science and Technology 2013* ed McGraw-Hill (New York, USA: McGraw-Hill Inc) p 281
[8] Olge P M *et al* 2004 *Astrophys. J* **606** 151
[9] Cassinelli J P *et al* 1981 *Astrophys. J* **250** 677
[10] Dutuit O *et al* 2013 *Astrophys. J* **204** 20
[11] Pérez-Montero E and Díaz A 2007 *Mon. Not. Roy. Astr. Soc.* **377** 1195
[12] Ignace R *et al* 2003 *Astron. Astrophys.* **408** 353
[13] Bohigas J 2005 *Astrophys. J* **674** 954

[14] Scully S W J, Álvarez I, Cisneros C, Emmons E D, Gharaibeh M F, Leitner D, Lubell M S, Müller A, Phaneuf R A, Püttner R, Schlachter A S, Schippers S, Ballance C P and McLaughlin B M 2006 *J. Phys. B: At. Mol. Opt. Phys.* **39** 3957

[15] Scully S W J, Álvarez I, Cisneros C, Emmons E D, Gharaibeh M F, Leitner D, Lubell M S, Müller A, Phaneuf R A, Püttner R, Schlachter A S, Schippers S, Ballance C P and McLaughlin B M 2007 *J. Phys. Conf. Ser.* **58** 387

[16] McLaughlin B M 2013 *J. Phys. B: At. Mol. Opt. Phys.* **46** 075204

[17] Müller A, Schippers S, Phaneuf R A, Scully S W J, Aguilar A, Cisneros C, Gharaibeh M F, Schlachter A S and McLaughlin B M 2010 *J. Phys. B: At. Mol. Opt. Phys.* **43** 135602

[18] Müller A, Schippers S, Phaneuf R A, Scully S W J, Aguilar A, Covington A M, Álvarez I, Cisneros C, Emmons E D, Gharaibeh M F, Schlachter A S, Hinojosa G and McLaughlin B M 2009 *J. Phys. B: At. Mol. Opt. Phys.* **42** 235602

[19] Müller A, Schippers S, Phaneuf R A, Scully S W J, Aguilar A, Cisneros C, Gharaibeh M F, Schlachter A S and McLaughlin B M 2014 *J. Phys. B: At. Mol. Opt. Phys.* in preparation for publication

[20] Scully S W J, Aguilar A, Emmons E D, Phaneuf R A, Halka M, Leitner D, Levin J C, Lubell M S, Püttner R, Schlachter A S, Covington A M, Schippers S, Müller A and McLaughlin B M 2005 *J. Phys. B: At. Mol. Opt. Phys.* **38** 1967

[21] Schlachter A S, Sant'Anna M M, Covington A M, Aguilar A, Gharaibeh M F, Emmons E D, Scully S W J, Phaneuf R A, Hinojosa G, Álvarez I, Cisneros C, Müller A and McLaughlin B M 2004 *J. Phys. B: At. Mol. Opt. Phys.* **37** L103

[22] Kawatsura K *et al* 2002 *J. Phys. B: At. Mol. Opt. Phys.* **35** *4147*

[23] Yamaoka H *et al* 2001 *Phys. Rev.* **A 65** *012709*

[24] Sant'Anna M M, Schlachter A S, Öhrwall G, Stolte W C, D W Lindle D W and McLaughlin B M 2011 *Phys. Rev. Letts.* **107** *033001*

[25] Krause M O 1994 *Nucl. Instr. and Meth. in Phys. Res. B* **87** 178

[26] Menzel A, Benzaid S, Krause M, Caldwell C D, Hergenhahn U and Bissen M 1996 *Phys. Rev. A* **54** R991

[27] Stolte W C, Samson J A R, Hemmers O, Hansen D, Whitfield S B and Lindle D W 1997 *J. Phys. B: At. Mol. Opt. Phys.* **30** 4489

[28] McLaughlin B M, Ballance C P, Bown K P, Gardenghi D J and Stolte W C 2013 *Astrophys. J* **771** L8

[29] Burke P G and Berrington K A 1993 *Atomic and Molecular Processes: An R-matrix Approach* (Bristol, UK: IOP Publishing)

[30] Berrington K A, Eissner W and Norrington P H 1995 *Comput. Phys. Commun.* **92** 290 URL `http://amdpp.phys.strath.ac.uk/APAP`

[31] Bizau J M *et al* 2004 *Phys. Scr.* **T 110** 57

[32] Bizau J M *et al* 2005 *Astron. Astrophys.* **439** 387

[33] Wang Guo-Li and Zhou Xiao-Xin 2009 *Chinese Phys. B* **18** 3833

[34] Burke P G 2011 *R-Matrix Theory of Atomic Collisions: Application to Atomic, Molecular and Optical Processes* (New York, USA: Springer)

[35] Petrini D and de Araújo F X 1997 *Astron. & Astrophys.* **326** 870

[36] Petrini D 1981 *J. Phys. B: At. Mol.* **14** 3839

[37] Stoica S, Petrini D and Bely-Dubau F 1998 *Astron. & Astrophys.* **334** L26

[38] Garcia J, Kallman T R, Witthoeft M, Behar E, Mendoza C, Palmeri P, Quintet P, Bautista M and Klapisch M 2009 *Astrophys. J Supp. Ser.* **185** 477

[39] Robicheaux F, Gorczyca T W, Griffin D C, Pindzola M S and Badnell N R 1995 *Phys. Rev. A* **52** 1319

[40] Verner D A *et al* 1993 *At. Data Nucl. Data Tables* **55** 233

[41] Verner D A and Yakovlev D G 1995 *Astron. Astrophys. Suppl.* **109** 125

[42] Reilman R and Manson S T 1979 *Astrophys. J. Suppl. Ser.* **40** 815

[43] Chen M H and Crasemann B 1987 *Phys. Rev A* **35** 4579

[44] Chen M H and Crasemann B 1988 *At. Dat. Nucl. Dat. Tables* **38** 381

[45] Bruneau J 1984 *J. Phys. B: At. Mol. Phys.* **17** 3009

[46] Sakho I *et al* 2013 *At. Data. Nuc. Data Tables* **99** 447

[47] Sakho I *et al* 2013 *Phys. Scr.* **88** 035302

[48] Travnikova O *et al* 2010 *Phys. Rev. Letts.* **105** 233001

[49] Miron C *et al* 2013 URL `http://www.synchrotron-soleil.fr/portal/page/portal/Recherche/LignesLumiere/PLEIADES`

[50] Sodhi R N S and Brion C E 1977 *J. Electron Spectrosc. Relat. Phenom.* **34** 363

[51] Kato M *et al* 2007 *J. Electron Spectrosc. Relat. Phenom.* **160** 39

[52] Miron C *et al* 2012 *Nature Phys.* **8** 135
[53] Kimberg V *et al* 2013 *Phys. Rev. X* **3** 011017
[54] Ballance C P and Griffin D C 2006 *J. Phys. B: At. Mol. Opt. Phys.* **39** 3617
[55] McLaughlin B M and Ballance C P 2012 *J. Phys. B: At. Mol. Opt. Phys.* **45** 085701
[56] McLaughlin B M and Ballance C P 2012 *J. Phys. B: At. Mol. Opt. Phys.* **45** 095202
[57] Clementi E and Roetti C 1974 *At. Data Nucl. Data Tables* **14** 177
[58] Berrington K, Quigley L, and Zhang H L 1997 *J. Phys. B: At. Mol. & Phys.* **30** 5409
[59] Hibbert A 1975 *Comput. Phys. Commun.* **9** 141
[60] Fano U and Cooper J W 1968 *Rev. Mod. Phys.* **40** 441
[61] Shore B W 1967 *Rev. Mod. Phys.* **39** 439
[62] Wright J D *et al* 2008 *Phys. Rev. A* **77** 062512
[63] Quigley L and Berrington K A 1996 *J. Phys. B: At. Mol. Phys.* **29** 4529
[64] Quigley L, Berrington K A and Pelan J 1998 *Comput. Phys. Commun.* **114** 225
[65] Ballance C P, Berrington K A and McLaughlin B M 1999 *Phys. Rev. A* **60** R4217
[66] Kramida A E, Ralchenko Y, Reader J, and NIST ASD Team (2013), NIST Atomic Spectra Database (version 5.1), National Institute of Standards and Technology, Gaithersburg, MD, USA URL `http://physics.nist.gov/PhysRefData/ASD/levels_form.html`
[67] Sun Y *et al* 2013 *Eur. Phys. J. D* **67** 88
[68] Guo-Li W and Xiao-Xi Z 2007 *Chinese Phys.* **16** 2361
[69] Sun Y, Chen F and Gou B C 2011 *J. Chem. Phys.* **135** 124309
[70] Daltabuit E and Cox D P 1972 *Astrophys. J.* **177** 855
[71] Slater J C 1930 *Phys. Rev.* **36** 57
[72] Slater J C 1960 *Quantum Theory of Atomic Structure, Vol 1* (New York, USA: McGraw-Hill)
[73] Bethe H A and Salpeter E E 1957 *Quantum Mechanics of One- and Two-Electron Systems* (New York, USA: Academic Press)
[74] Gatuzz E *et al* 2013 *Astrophys. J* **768** 60
[75] Lin S -H, Hsue C - S and Chung K T 2001 *Phys. Rev. A* **64** 012709
[76] Lin S -H, Hsue C - S and Chung K T 2002 *Phys. Rev. A* **65** 032706
[77] Ferland G J, Korista K T, Verner D A, Ferguson J W, Kingdon J B and Verner E M 1998 *Pub. Astron. Soc. Pac.(PASP)* **110** 761
[78] Ferland G J 2003 *Ann. Rev. of Astron. & Astrophys.* **41** 517
[79] Kallman T R and Bautista M A 2001 *Astrophys. J. Suppl. Ser.* **134** 139
[80] Foster A R, Ji L, Smith R K and Brickhouse N S 2012 *Astrophys. J* **756** 128